Journal of Ceramic Processing Research. Vol. 15, No. 5, pp. 341~346 (2014)

J O U R N A L O F
Ceramic Processing Research

Preparation of graphite nanosheets by combining microwave irradiation and liquid-phase exfoliation

Ji Hwan Kim and Jong-Hyun Lee*
Department of Materials Science and Engineering, Seoul National University of Science and Technology, Seoul 139-743, Korea

We demonstrate a series of experiments involving pretreatment with acid-based solvents, microwave irradiation, and post treatment with organic solvents to prepare graphite nanosheets from graphite powders. It was confirmed by microstructural observation and XRD analysis that a 24 h acid pretreatment forms a graphite intercalation compound (GIC) and a 90 s microwave irradiation promotes exfoliation behavior during transformation into expanded graphite. In the post treatment with organic solvents (liquid-phase exfoliation), the average thickness of prepared graphite nanosheets was influenced dominantly by the surface energy (or surface tension) of the solvent. However, the yield of graphite nanosheets was strongly proportional to the solvent viscosity. The exfoliation of graphite with the series of experiments was successfully conducted and finally transformed into nanosheets with an average thickness of 2.86 nm and a yield of 80% by using 1-cyclohexyl-2-pyrrolidone in the liquid-phase exfoliation.

Key words: Intercalation, Exfoliation, Graphite nanosheets, Microwave irradiation, Liquid-phase exfoliation, Yield.

Introduction

With accelerated miniaturization and the high performance trend in the electronic packaging industry, the need to adopt novel materials has been increasing. Graphite is noted as an electronic packaging material due to its potentially high thermal conductivity, extremely low thermal expansion and weight, and low cost [1-3]. For this reason, studies on the preparation of graphite few-layer nanosheets, including graphene, have been extensive in recent years [3-5]. Although a high yield method to prepare graphene on a mass production basis by exfoliating graphite was not implemented industrially, chemical techniques preparing thin graphite nanosheets or fine graphite fragments became feasible through two representative approaches: exfoliation of graphite oxide [6] and nonoxidative exfoliation [7-13]. The nonoxidative exfoliation by use of an intercalant such as an acid [7-9], salt [10, 11], alkali metal [3, 12], or organic compound [13] was characterized as high quality and low yield, while the exfoliation process of graphite oxide needed an additional reduction process and inevitably created a significant number of defects and chemical functional groups [14]. The functional groups and defects disrupt the electronic properties [13], thus the method may be inappropriate for application as a functional electronic material. The best result achieved by nonoxidative exfoliation was obtained using N-methyl-pyrrolidone (NMP) solvent where monolayer graphite (graphene) was fabricated [13]. However, an overall yield (mass of monolayers/mass of starting graphite) of the monolayer graphite was just ~ 1 wt% [13]. Moreover, the manu-facturing yield of graphene or graphite nanosheet has not been identified in most reports.

Graphite nanosheets have been successfully applied in the electronic packaging field as a composite ad-hesive. Yu *et al*. reported that epoxy composites, which consisted of graphite nanosheets approaching full exfoliation, demonstrate a remarkable enhancement of the thermal conductivity in comparison to those containing slightly exfoliated graphite nanosheets, especially at high filler loadings [15]. Hence, the optimization of fabricating processes that approach the full exfoliation of graphite is urgently required. In summary, both yield and degree of exfoliation are important in the commercial fabrication of graphite nanosheets.

In this study, the exfoliation technique by the combination of pretreatment with acid-based solvents, microwave irradiation, and post treatment with organic solvents was conducted for effective full exfoliation of micron-scale graphite particles. First, the characteristics of the expanded graphite prepared with respect to microwave irradiation parameters after the pretreatment were surveyed and an optimal irradiation time was set. Next, the usefulness of post treatment with four types of organic solvents was investigated with two viewpoints for the average thickness and yield of nanosheets to fabricate effectively thinner graphite sheets.

Experimental Procedures

1 g of natural graphite powder (#3609, Asbury

*Corresponding author:
Tel : +82-2-970-6612
Fax: +82-2-973-6657
E-mail: pljh@seoultech.ac.kr

Graphite Mills, Inc., > 95%, average size: 75 μm) was added into 12 ml of a mixture (3 : 1 by volume) of sulfuric acid (> 96%) and nitric acid (96%) and stored for 24 h at room temperature. The graphite intercalation compound (GIC) in the acid mixture was filtered using a funnel type filter with pores of 10-16 μm diameter. During filtration, the GIC was washed repeatedly with distilled water and then air dried under a hood for 48 h. The dried GIC was then expanded by microwave irradiation. The power was set at 800 W and the exfoliation result was evaluated as a function of irradiation time. The GIC caught fire abruptly during the irradiation.

Because the degree of exfoliation by microwave irradiation was not satisfactory, the exfoliation process was followed by sonication with various organic solvents and then centrifugation (liquid-phase exfo liation) for 30 min each. The centrifugation was performed at 500 rpm. Five solvents were selected as the organic solvent: acetone (Samchun Chemicals, the or, 1-methyl-2-pyrrolidinone (1M2P, Sigma-Aldrich, 99.5%), 1-cyclohexyl-2-pyrrolidone (1C2P, Aldrich, 99%), 1-vinyl-2-pyrrolidinone (1V2P, Aldrich, ≥ 99%), and dimethyl sulfoxide (DMSO, Sigma-Aldrich, ≥ Sigma). All solvents were used as received.

The appearance of graphite prepared after each exfoliation step was examined using a scanning electron microscope (SEM, S-2300, Hitachi) or a transmission electron microscope (TEM, Tecnai 20, FEI Co.). The homogeneous dispersion (supernatant) prepared after the centrifugation was dripped on a copper grid and dried to prepare TEM samples. To compare with pristine graphite powder, the GICs before and after the microwave irradiation were also measured by X-ray diffraction (XRD) with a diffractometer (X'pert MPD, Philips) using CuK_α radiation. A drop of the dispersion of exfoliated graphite (graphite nanosheet) was dripped on a glass substrate and dried and the thickness of each nanosheet was quantitatively studied by tapping mode atomic force microscopy (AFM, Nanoscope IV, Digital Instrument). The number of measured nanosheets was 50 for each type of solvent.

We calculated the total yield of graphite nanosheets (the mass of dispersed graphite / the mass of initial graphite powder, $W_{nanosheet}$ / W_{powder}) from:

$$\frac{W_{nanosheet}}{W_{powder}} = \frac{W_{powder} - W_{sediment}}{W_{powder}}$$

where $W_{sediment}$ represents the weight in the dried state of sediment powder after the centrifugation.

Results and Discussion

Preparation of expanded graphite by microwave irradiation after pretreatment with an acid mixture

Fig. 1 shows SEM micrographs of pristine graphite powder and GIC, which was prepared by the acid treatment. The GIC exhibited a pastry-like structure having the layer planes cleaved with a sub-micrometer width, while the pristine graphite was a dense aggregate of stratums. This suggests that the acid pretreatment facilitated the intercalation of the pristine graphite. The structural change is believed to be induced by drying the acid intercalants after the immersion in an acid mixture.

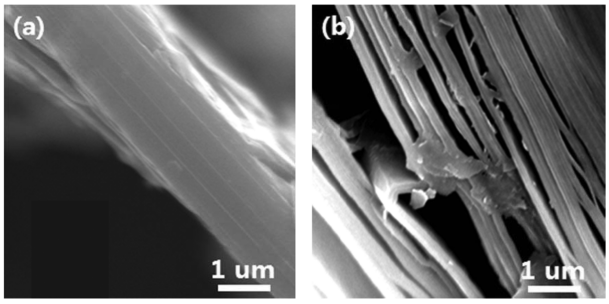

Fig. 1. SEM images of (a) pristine graphite and (b) graphite intercalated compound after acid treatment.

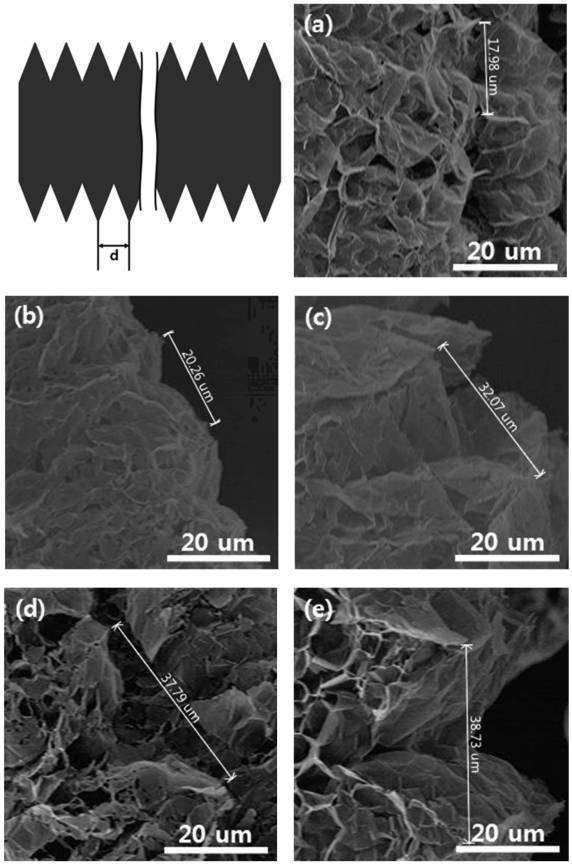

Fig. 2. Schematic diagram and SEM images of accordion-like graphite particle expanded after microwave irradiation. The SEM images show graphite prepared after irradiation for (a) 10 s, (b) 30 s, (c) 50 s, (d) 70 s, and (e) 90 s. The d value is labeled in each image.

Fig. 2 exhibits the SEM images of expanded graphite with respect to microwave irradiation time. The microwave irradiation induced major morphological changes of the GIC that was prepared by the acid mixture

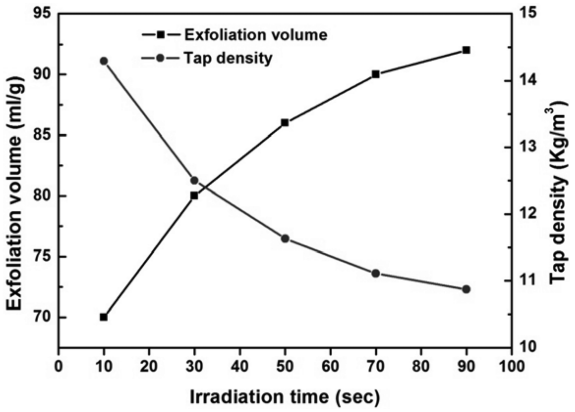

Fig. 3. Correlation between microwave irradiation time and expansion volume of graphite prepared by microwave irradiation.

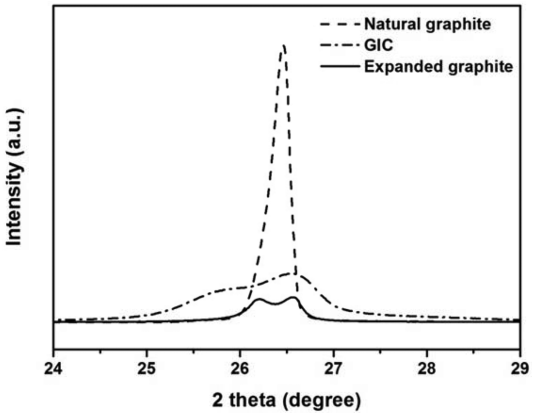

Fig. 4. XRD patterns within the range 24-29 º of (a) pristine graphite, (b) graphite after pretreatment with acid mixture, and (c) graphite expanded by microwave irradiation.

treatment, finally forming expanded graphite with an accordion-like structure. The microwave irradiation stimulates intercalates (acid molecules) in the GIC and rapidly generated heat causes the vaporization and violent expulsion of some intercalates. Hence, the vaporization pressure can exfoliate the carbon layers of graphite if the pressure is higher than the van der Walls interaction between the carbon layers. The degree of expansion with irradiation time can be estimated as the variation of distance between peaks in the accordion-like structure [16]; this is named the d value in Fig. 2. As a result, the d value increased with increasing irradiation time, indicating an increase in the degree of expansion. Since the initial concentration of volatile intercalate in the GIC was identical, the longer irradiation time would lead to a larger amount of vaporized intercalates. A larger amount of vaporized intercalates per unit volume in the compounds during irradiation should show a larger expansion volume. However, since the amount of intercalates in the compound is finite, the increase of expansion volume will be saturated as intercalates are consumed by evaporation.

In order to quantitatively evaluate the degree of expansion with respect to the irradiation time, the volume and tap density of expanded graphite were measured and are summarized in Fig. 3. The volume was determined for 1.0 g of expanded graphite and measured using a mesh cylinder. The tap density was inversely calculated from the expansion volume. The expansion volume clearly increased with irradiation time and consequently the tap density decreased. Moreover, the rate of the volume increase with irradiation time saturated proving the above-mentioned discussion that the finite amount of intercalates in the GIC would be gradually consumed by evaporation.

The XRD patterns of the acid treated GIC and expanded graphite irradiated for 90 s are displayed in Fig. 4 in comparison with that of pristine graphite powder. The pristine graphite showed a very strong and sharp (002) reflection detected at 26.45 º [7]. However, the GIC showed a broad diffraction peak at 25.77 º in addition to a weaker and broader peak at 26.55 º. The novel peak was attributed to an increased interlayer spacing by acid intercalation [7]. This result indicates there is partial intercalation of graphite by the acid after the 24 h storage. Meanwhile, the slight peak shift to 26.55 º would be attributed to a decreased interlayer spacing. A microstrain effect by the entrance of acid intercalant into the edge of the layers might induce layer warpage, resulting in an increase of interlayer spacing at the edge region and a corresponding slight decrease in the interlayer spacing at the center region [17].

After microwave irradiation, the broad peak at 25.77 º disappeared and another peak formed at 26.20 º. The sudden temperature increase by microwave irradiation leads to the vaporization and violent expulsion of acid, causing the exfoliation of graphite, which explains the volume increase and disappearance of the 25.77 º peak. However, the intercalation effect by residual acid was still observed with the 26.20 º peak. The intensity of the peaks observed after microwave irradiation was greatly reduced, indirectly, but evidently, indicating that successful exfoliation is promoted by microwave irradiation. However, it was also observed that the exfoliation was partial and insufficient. Thus, an additional liquid-phase exfoliation step was required in order to enhance the yield of graphite nanosheets via more effective exfoliation and divide the accordion-like structure into nanosheets.

Preparation of graphite nanosheets by liquid-phase exfoliation as post treatment

Fig. 5 shows the bright-field TEM images of exfoliation-treated graphite nanosheets with respect to the type of organic solvents used after a microwave irradiation of 90 s. Though most of the graphite nanosheets were folded or overlapped, the lateral size was typically a few micrometers (Fig. 5a). Each plane in the graphite nanosheet was observed distinctly in the

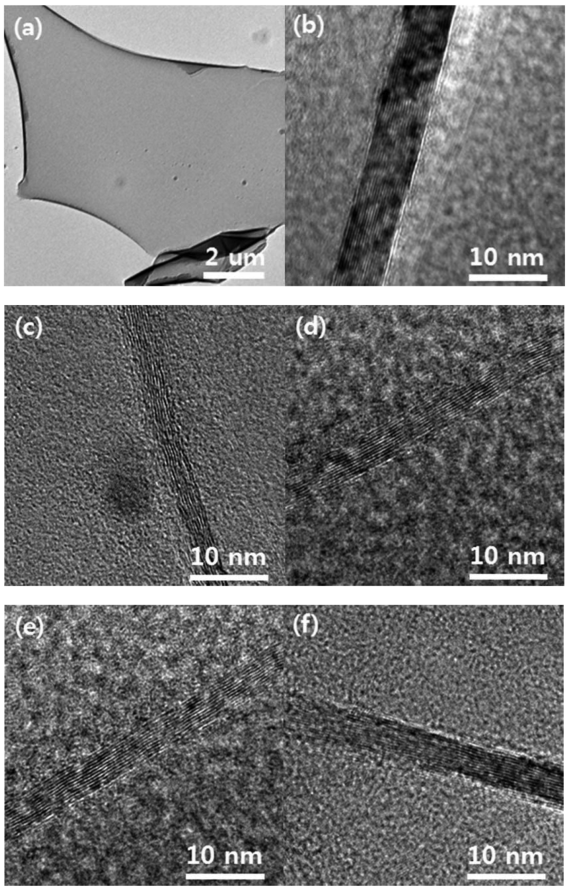

Fig. 5. Bright-field TEM micrographs showing (a) a plane image of graphite nanosheet typically observed after post treatment and cross-sectional images of graphite nanosheets post treated with (b) acetone, (c) 1M2P, (d) 1C2P, (e) 1V2P, and (f) DMSO.

cross-sectional images. However, the observed thickness of graphite nanosheets was different with the type of used organic solvents used.

Fig. 6 shows histograms of the number of layers per graphite nanosheets with different solvent type, which are measured by AFM. The number of layers per sheet could be calculated by dividing the measured thickness with the graphitic interlayer spacing (0.34 nm) and the histogram was displayed with the interval of five layers. All samples showed the highest frequency at 1-5 or 6-10 layers, although the frequency distribution was different in each histogram. The graphite nanosheets post treated with acetone showed a multilayer structure with an average thickness of around 4.14 nm. Meanwhile, the graphite nanosheets processed with 1M2P, 1C2P, 1V2P, and DMSO displayed multilayered structures having an average thickness of 2.40 nm (± 2.42 nm), 2.86 nm (± 2.37 nm), 3.06 nm (± 1.79 nm), and 3.08 nm (± 2.20 nm), respectively, which are thinner than that of acetone. This result corresponded well with the microstructural observation of Fig. 5. Consequently, the four solvents showed increased exfoliation performance compared to acetone. In addition, 1M2P and 1C2P indicated the highest degree of exfoliation among the

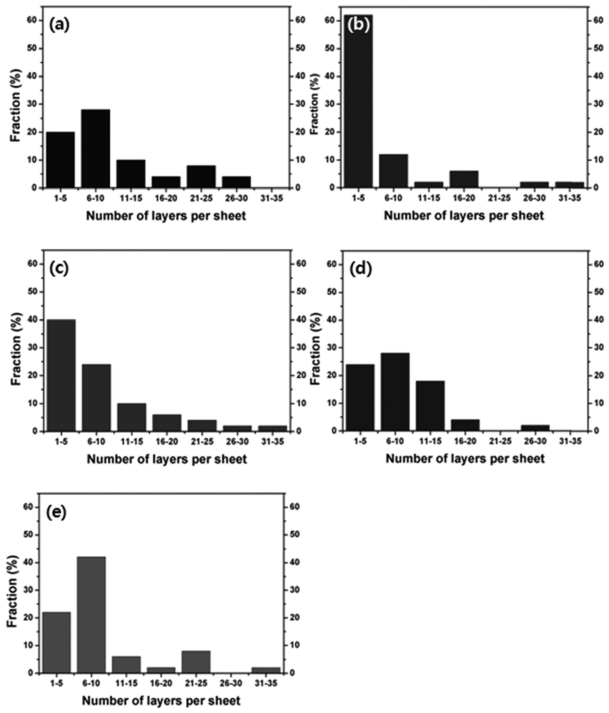

Fig. 6. Histograms of the number of layers per graphite nanosheet post treated with (a) acetone, (b) 1M2P, (c) 1C2P, (d) 1V2P, and (e) DMSO.

used solvents.

Hernandez *et al*. suggested solvent surface energy (or surface tension) as the most influential property leading to the exfoliation of graphite in liquid-phase exfoliation because the enthalpy of mixing is dependent on the balance of graphene and solvent surface energies [13]. Thus the surface tension of the five solvents used in this study were measured by the standard Wilhelmy plate technique [18] using a surface tensiometer (K11, Kruss) and the results are shown in Fig. 7 in comparison with the average thickness of the graphite nanosheet calculated from Fig. 6. The exfoliation was clearly enhanced with a solvent surface tension of 39.16 mJ/m^2, whereas it was inactive with acetone having a lower surface tension of 23.25 mJ/m^2. In the previous liquid-phase exfoliation experiments [13], exfoliation behaviors occurred mostly with surface tensions ranging from ~ 34-46 mJ/m^2 and solvent surface energies, calculated from the surface tension, very close to the literature values of graphite surface energy. They insisted that such exfoliation could occur when the net energetic cost of exfoliation is minimal for the solvent whose surface energy matches that of graphene [13]. Thus, the surface tension range indicating strong interaction between the solvent and graphite in our study coincided well with previous studies.

Besides the thickness of exfoliated graphite, the yield of graphite nanosheets homogeneously dispersed in the solvent, except for the sediments after centrifugation, is also an important factor to investigate. Table 1 shows

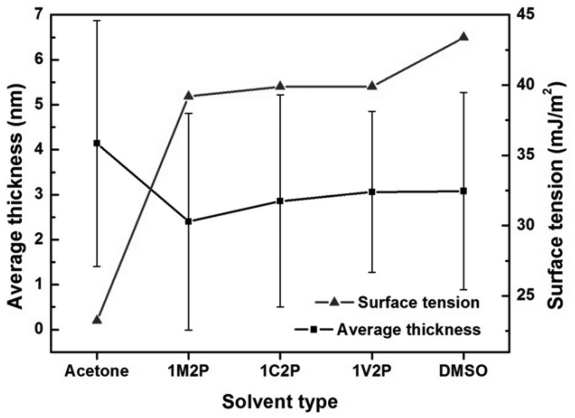

Fig. 7. Relationship between the average thickness of graphite nanosheets dispersed in solvent and the surface tension of the solvent displayed as a function of solvent type.

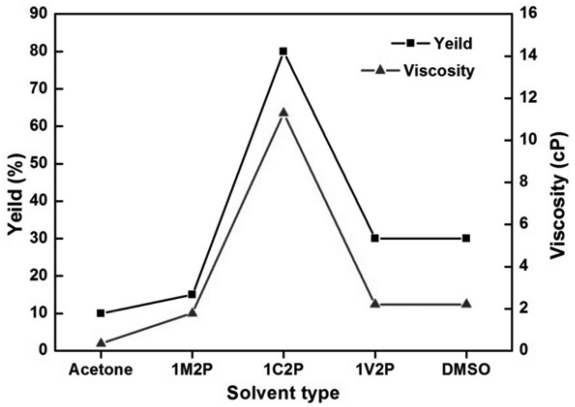

Fig. 8. Relationship between the yield of thin graphite nanosheets and the solvent viscosity displayed as a function of solvent type.

Table 1. Yield of graphite nanosheets and viscosity measured with respect to solvent type.

Solvent	Yield (%)	Viscosity (cP)
Acetone	10	0.34
1-methyl-2-pyrrolidinone	15	1.78
1-cyclohexyl-2-pyrrolidone	80	11.29
1-vinyl-2-pyrrolidinone	30	2.19
Dimethyl sulfoxide	30	2.19

the yield of nanosheets obtained from the pristine graphite with a different solvent type. 1C2P represented an outstanding yield of 80%, which was the highest value among solvents, whereas the others showed a poor yield of 10-30%. Despite the fact that graphite nanosheets prepared in 1M2P represented the thinnest average thickness, as shown in Fig. 5 and 6, the yield in 1M2P was much lower than that in 1C2P. Thus, the yield data had no correlation with the thickness results from exfoliated graphites. Consequently, 1M2P could be considered the best solvent used in this study simultaneously considering the average thickness and yield of the nanosheets.

Viscosity values of the solvents used are also summarized in Table 1. A digital Brookfield viscometer (RVDV-II + P) was used to measure viscosity. The relationship between yield and solvent viscosity is shown in Fig. 8. The outstandingly high yield obtained with 1C2P corresponded well with its extremely high viscosity of 11.29 cP. The low yields in the other solvents were linked to low viscosity values, indicating that yields are strongly related to solvent viscosity. Hence, the solvent viscosity can be considered a crucial factor influencing the homogeneity of exfoliation during the liquid-phase treatment and finally the yield of graphite nanosheets.

Conclusions

By a series of experiments involving pretreatment with acid-based solvents, microwave irradiation, and post treatment with organic solvents, the exfoliation of graphite was successfully conducted and pristine graphite powders were transformed into nanosheets. It was observed by microstructural observation and XRD analysis that the acid pretreatment forms GIC and the microwave irradiation promotes the intercalation behavior during the transformation of GIC into expanded graphite. The degree of expansion (intercalation) increased and saturated by increasing irradiation time to 90 s. In the post treatment with organic solvents (liquid-phase exfoliation), it was proven that the average thickness of prepared graphite nanosheets is influenced by the surface energy (or surface tension) of the solvent and the surface tension ranging from 34-46 mJ/m^2 is favorable for exfoliation. However, it was found that the yield of graphite nanosheets, having no connection with the trend in thickness, is strongly proportional to the solvent viscosity. Thus highly viscous 1-cyclohexyl-2-pyrrolidone, having a surface tension of 39.88 mJ/m^2, was considered an effective solvent in the liquid-phase exfoliation.

Acknowledgments

The authors thank the Seoul center of Korea Basic Science Institute (KBSI) for SEM and TEM measurement.

References

1. J. Li, M.L. Sham, J.-K. Kim, G. Marom, Compos. Sci. Technol. 67 [2] (2007) 296-305.
2. J. Li, J.-K. Kim, Compos. Sci. Technol. 67 [10] (2007) 2114-2120.
3. L.M. Viculis, J.J. Mack, O.M. Mayer, H.T. Hahn, R.B. Kaner, J. Mater. Chem. 15 [9] (2005) 974-978.
4. B. Li, W.-H. Zhong, J. Mater. Chem. 46 [17] (2011) 5595-5614.

5. R.S. Edwards, K.S. Coleman, Nanoscale 5 [1] (2013) 38-51.
6. X. Fan, W. Peng, Y. Li, X. Li, S. Wang, G. Zhang, F. Zhang, Adv. Mater. 20 [23] (2008) 4490-4493.
7. T. Wei, Z. Fan, G. Luo, C. Zheng, D. Xie, Carbon 47 [1] (2009) 337-339.
8. S. Malik, A. Vijayaraghavan, R. Erni, K. Ariga, I. Khalakhan, J.P. Hill, Nanoscale 2 [10] (2010) 2139-2143.
9. W. Gu, W. Zhang, X. Li, H. Zhu, J. Wei, Z. Li, Q. Shu, C. Wang, K. Wang, W. Shen, F. Kang, D. Wu, J. Mater. Chem. 19 [21] (2009) 3367-3369.
10. W. Fu, J. Kiggans, S.H. Overbury, V. Schwartz, C. Liang, Chem. Commun. 47 [18] (2011) 5265-5267.
11. A. Safavi, M. Tohidi, F.A. Mahyari, H. Shahbaazi, J. Mater. Chem. 22 [9] (2012) 3825-3831.
12. C. Valles, C. Drummond, H. Saadaoui, C.A. Furtado, M. He, O. Roubeau, L. Ortolani, M. Monthioux, A. Penicaud, J. Am. Chem. Soc. 130 [47] (2008) 15802-15804.
13. Y. Hernandez, V. Nicolosi, M. Lotya, F.M. Blighe, Z. Sun, S. De, I.T. Mcgovern, B. Holland, M. Byrne, Y.K. Gunko, J.J. Boland, P. Niraj, G. Duesberg, S. Krishnamurthy, R. Goodhue, J. Hutchison, V. Scardaci, A.C. Ferrari, J.N. Coleman, Nat. Nanotechnol. 3 [9] (2008) 563-568.
14. D.R. Dreyer, S. Park, C.W. Bielawski, R.S. Ruoff, Chem. Soc. Rev. 39 [1] (2010) 228-240.
15. A. Yu, P. Ramesh, M.E. Itkis, E. Bekyarova, R.C. Haddon, J. Phys. Chem. C 111 [21] (2007) 7565-7569.
16. F. Kang, Y.-P. Zheng, H.-N. Wang, Y. Nishi, M. Inagaki, Carbon 40 [9] (2002) 1575-1581.
17. J.-S. Park, M.-H. Lee, I.-Y. Jeon, H.-S. Park, J.-B. Baek, H.-K. Song. ACS Nano 6 [12] (2012) 10770-10775.
18. E. Rame, J. Colloid Interface Sci. 185 [1] (1997) 245-251.